



ELSEVIER

Applied Catalysis A: General 178 (1999) 177–189



Preparation of high loading silica supported nickel catalyst: simultaneous analysis of the precipitation and aging steps

Márcio Nele, Adriana Vidal, Daniel L. Bhering, José Carlos Pinto, Vera Maria M. Salim*

Programa de Engenharia Química/COPPE, Universidade Federal do Rio de Janeiro, Cidade Universitária, CP:68502, Rio de Janeiro, 21945-970 RJ, Brazil

Received 23 February 1998; received in revised form 3 August 1998; accepted 5 August 1998

Abstract

The precipitation and aging steps used for the preparation of high loading silica supported nickel catalysts were simultaneously analyzed with the aid of statistical design of experiments. Empirical models relating catalyst final properties and preparation variables were developed. It was found that the precipitation step determines the final catalyst nickel content, and that at low nickel concentrations high metallic area per gram of reduced nickel may be attained with the precipitated precursor without performing the aging step. When it is performed, the aging step has a strong influence on final catalyst properties, such as specific surface area, metallic area per gram of nickel and degree of reduction. Therefore, catalyst aging may be an effective method to control dispersion, reducibility and active phase accessibility. The importance of the aging step was shown to increase with the aging temperature, which is linked to the larger rates of silicate formation at high temperatures. A semi-empirical model was developed to describe the final catalyst specific surface area as a function of the rate of silicate formation. This model is able to describe changes of the catalyst surface area fairly well and allow the proper manipulation of preparation conditions in order to maximize the catalyst specific area, leading to maximum catalyst activities. © 1999 Elsevier Science B.V. All rights reserved.

Keywords: Nickel catalyst; Catalyst preparation; Design of experiments; Silica supported catalyst

1. Introduction

Silica supported nickel catalysts are used extensively in many industrial processes such as hydrogenation of edible oils and aromatics in distillate fuels. As all these catalysts require optimized physical and chemical properties, a great deal of research has been reported with the aim of developing controlled catalyst preparations. Continuous efforts are made and

literature presents numerous works relating preparation methods, catalysts structure and catalytic behavior [1–4]. Studies developed by Schuit and van Reijen [5], Coenen and Linsen [6,7] and Geus et al. [8,9] may be regarded as fundamental landmarks in this field.

The “change-one-factor-at-a-time method” [10–13] was used previously to study the characteristics of high loading nickel catalysts used for hydrogenation of edible oils. The influence of the carrier textural properties, nickel loading and precipitating agent on

*Corresponding author. E-mail: vera@peq.coppe.ufrj.br

the metallic dispersion and on the metal–silica interaction was investigated using deposition-precipitation (DP) methods [10,11]. The influence of the precipitation temperature and aging conditions, that determine the nuclei formation rate, the growth of nickel crystallites and the rate of nickel silicate formation, were also studied [12]. As it is well known that hydrogenation of edible oils is a structure insensitive reaction [6,7], the catalytic activity depends mostly on the metal surface area and catalyst site accessibility. Therefore, the aging step was then optimized in order to allow the obtaining of a satisfactory metal surface area and good accessibility to the catalysts sites (pore diameters above 50 Å) [13]. The results obtained demonstrated that the metallic area and textural properties are strongly affected by the aging conditions and that the DP method can allow the preparation of very different catalysts by just adjusting aging time and temperature. The nickel silicate formation was analyzed and the nickel antigorite silicate identification was performed by DRX, ATG, XPS and TPR [13]. However, as each variable effect was studied independently of the other ones, variable interactions could not be detected in these previous studies and global optimization of catalyst preparation could not be carried out. Besides, as variables were not allowed to vary simultaneously, no attempts were made to build a mathematical model to describe the catalyst preparation.

Although statistical techniques have been successfully applied in the field of quality engineering, the vast majority of the experimental work performed for the preparation of catalysts uses the “change-one-factor-at-a-time” method. According to this method, effects are analyzed by varying one variable (factor) and keeping all other variables fixed at a specified set of conditions. The open literature has only few reports on the use of statistical design of experiments to catalyst preparation. Rouiller and Assaf [14] used a central composite design to investigate the influence of the preparation conditions on the metallic area and catalytic activity to cyclohexane deshydrogenation of the Ni/Al₂O₃ catalyst. Baker et al. [15] used a Plackett–Burman matrix to study the preparation of Cu/Co/Zn/Al catalysts. Lima et al. [16] successfully applied mixture designs to investigate the influence of the composition on the catalytic properties of Cu/ZnO/Al₂O₃ in the water gas shift reaction. Dawson and

Barnes [17] applied the Taguchi method to optimize the preparation of a copper–carbon catalyst.

The popularity of the “change-one-factor-at-a-time” method can be explained by its simplicity and the few numbers of experiments needed to study the influence of the factor (if k factors are analyzed, a minimum number of $k+1$ experiments would have to be carried out). However, in practice many more than $k+1$ experiments are usually needed. The simplicity of this method is misleading and can lead to unreliable results and wrong conclusions [18]. If one has a set of variables (e.g. A, B, C, D) and estimates the effect of A , keeping B, C and D at fixed values, the observed effect is guaranteed to be correct only when B, C and D are constant and equal to the fixed values. So, there is no guarantee whatsoever that the effect of A will remain the same when one of the other conditions changes. Besides, this method does not allow the observation of possible non-linear interaction effects among variables, as variables do not change simultaneously.

It is well known in heterogeneous catalysis that variables can interact with each other and produce unexpected results. Given the complex set of physical and chemical phenomena that occur during catalyst preparation, preparation variables, such as precipitation temperature, concentration of salts, aging time and temperature, calcination temperature, etc., probably interact among themselves, which may lead to unexpected results. The use of statistical experimental designs, especially factorial designs, can lead to much more consistent results in this case, as single variable effects are obtained as averages over the whole experimental region of interest, as all other factors change simultaneously. The use of proper statistical experimental designs also allows the computation of non-linear interactions, which may then be compared to the single variable effects, as interactions are often more important than single effects.

The “change-one-factor-at-a-time” strategy usually lets the researcher free to select the experimental conditions for experimentation, and decisions rely greatly on previous experience. By using statistical design of experiments, experimental conditions are specified in order to maximize the amount of information (effects are computed with minimum uncertainty) that can be obtained with minimum experimental effort. As optimum experimental condi-

tions depend on the modeling approach, it is assumed that the researcher is also interested in providing quantitative interpretation for variable effects. Given the target model and the experimental region of interest, optimum experimental conditions may be tabulated as functions of the number of experiments in a table called matrix of experiments or design matrix.

The methodology that one may use to investigate catalyst preparation procedures using the statistical design of experiments can be described in the following steps:

1. Selection of the response variables to be investigated. In heterogeneous catalysis these variables usually are final physico-chemical properties that characterize the catalyst performance (e.g. metallic area, surface composition, etc.) or a specific reaction rate per catalyst unit.
2. Identification of the preparation variables that may influence the selected response variables.
3. Selection of a target model and maximum number of experiments. The target model may be derived theoretically (which is rare in the catalyst field) or empirically, usually presenting the form:

$$y = b + \sum_{i=1}^n a_{ii}x_i + \sum_{i=1}^n \sum_{j=2, j>i}^n a_{ij}x_i x_j, \quad (1a)$$

where the independent variables (x_i) are the preparation variables, usually normalized to be within the interval $[-1, 1]$ as

$$x = \frac{z - ((z_{\max} + z_{\min})/2)}{(z_{\max} - z_{\min})/2}, \quad (1b)$$

where z are the actual variable values and the subscripts max and min stand for the maximum and minimum values used for experimentation; the dependent variable (y) is the selected response; n is number of independent variables; b is the independent term; a_{ii} and a_{ij} are the regression coefficients related to the main effects and to the second-order interactions, respectively. The maximum number of experiments must be larger than the number of model parameters.

4. Selection of adequate number of levels (allowed experimental values) for each preparation variable. Usually two levels are enough to begin a study.
5. Selection of the matrix of experiments based on the target model, the number of preparation variables

regarded as relevant, the number of levels for each preparation variable, and the maximum number of experiments that can be carried out.

6. Inclusion of additional central point experiments (usually 3–5 replicates) to allow the estimation of the experimental error.
7. Carrying out of selected experiments.
8. Analysis of experimental data using regression procedures. If the values of the variables x_i are normalized in the range $[-1, +1]$, the effects of the single variables and their interactions can be compared to each other in order to allow the identification of most significant effects and the interpretation of the experimental results.
9. Discarding of variables that are not significant and building of a mathematical model that relates the response and the statistically significant variables.
10. Checking whether the model is able to represent the response y within the experimental error.

If some sort of optimization is intended, the model can be used to allow the selection of the experimental conditions which leads to the maximization (minimization) of the specified objective function. In this case, an additional validation experiment should be carried out to confirm the prediction or allow the correction of the model and the prediction of a new optimum experimental condition.

In this work a rigorous study of the deposition–precipitation (DP) method is developed for high loading nickel catalyst using FC Celite as support and bicarbonate ions as precipitating agent. Preparation variables were investigated simultaneously in order to determine their relative influence and identification of possible interactions. Research efforts are concentrated on the study of the simultaneous influence of precipitation and aging conditions (keeping calcination and reduction conditions constant) on the final nickel loading, specific surface area, reducibility and metallic surface of the Ni/SiO₂ catalyst. The main objective here is selecting the preparation conditions that allow the maximization of the catalyst metallic surface area, while keeping good accessibility to catalyst sites (pore diameters above 50 Å), leading to maximum catalyst activity [10–13]. Preparation variables that are believed to influence the final physico-chemical properties of the Ni/SiO₂ catalyst are shown in Fig. 1.

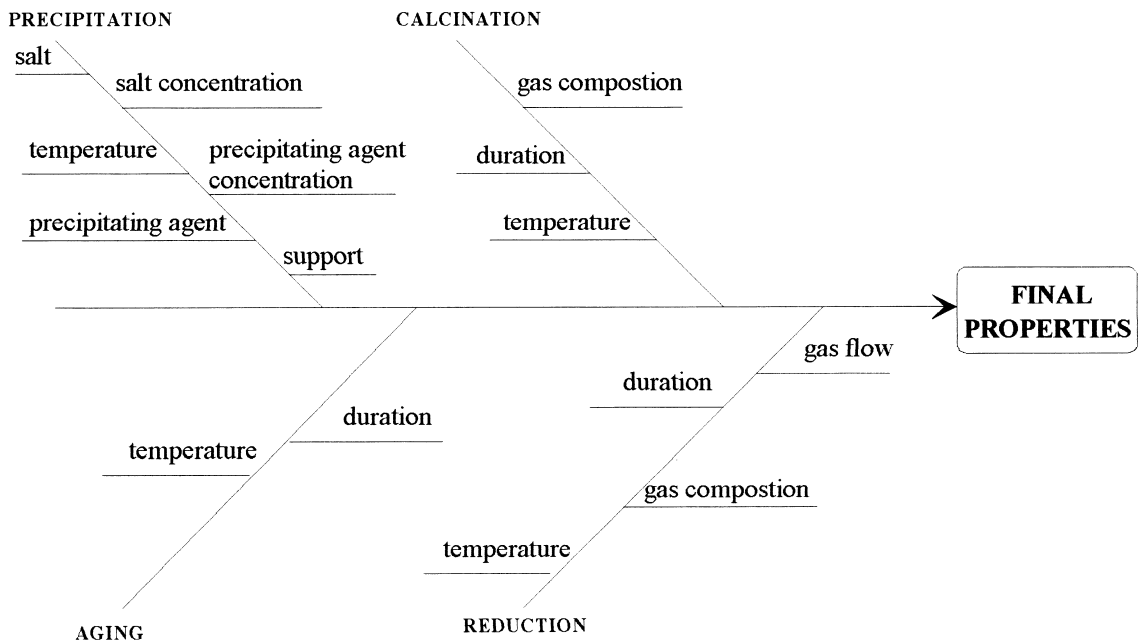


Fig. 1. Preparation variables for Ni/SiO₂ catalysts.

2. Experimental

2.1. Preparation of the catalysts

Catalysts precursors were prepared using a deposition–precipitation method. The precipitation of nickel was induced by slow addition of NaHCO₃ to a slurry containing the silica carrier (a diatomaceous earth FC Celite–Manville, 1% of alumina, 42 m²/g and $V_p=1.1$ cm³/g) and nickel nitrate solution. Different precipitation and aging conditions were used. The list of variables investigated is shown in Table 1. The design matrix is shown in Table 2 (experimental conditions are normalized in the range [−1,+1]).

Table 1
Real and coded values of experimental variables

Variable	Coded variable	Lower value (−1)	Central value (0)	Upper value (+1)
Nominal nickel content (%)	Ni*	20	30	40
Precipitation temperature (K)	T_p^*	298	330	363
Aging temperature (K)	T_a^*	298	330	363
Aging time (h)	t_a^*	0	10	20
Agitation	W^*	Low	Mean	High
NiNO ₃ concentration (M) ^a	Conc*	0.4	0.6	0.8

^ain the slurry.

After precipitation, the material was aged, filtered, washed and dried at 373 K (20 h). Afterwards, it was calcinated in two stages: in the first stage it was calcinated at 573 K during 3 h (573 K) and in the second stage at 723 K during 2 h.

2.2. Design of experiments

The relative importance of single variable and interaction effects was investigated by using a Taguchi design, which is a fraction of the full factorial design. A design matrix with 16 experiments and six variables was selected as shown in Table 2. Four central experiments (experiments 17–20) were added to the design

Table 2
Matrix of experiments

Experiment	Ordering ^a	Ni*	Tp*	Ta*	ta*	W*	Conc*
1	10	-1	-1	-1	-1	-1	-1
2	4	-1	-1	-1	+1	-1	+1
3	16	-1	-1	+1	-1	+1	-1
4	6	-1	-1	+1	+1	+1	+1
5	14	-1	+1	-1	-1	-1	-1
6	1	-1	+1	-1	+1	-1	+1
7	20	-1	+1	+1	-1	+1	-1
8	15	-1	+1	+1	+1	+1	+1
9	5	+1	-1	-1	-1	+1	+1
10	9	+1	-1	-1	+1	+1	-1
11	19	+1	-1	+1	-1	-1	+1
12	12	+1	-1	+1	+1	-1	-1
13	2	+1	+1	-1	-1	+1	+1
14	7	+1	+1	-1	+1	+1	-1
15	18	+1	+1	+1	-1	-1	+1
16	13	+1	+1	+1	+1	-1	-1
17,18,19,20	3,8,11,17	0	0	0	0	0	0

^a After randomization.

matrix in order to allow the evaluation of the experimental error. Experimental conditions were selected in order to allow the computation of the interaction between aging time and aging temperature (assumed to be very important a priori). However the main effects of agitation and nickel nitrate concentration may be confounded with the interactions between nominal nickel content and aging temperature and nominal nickel content and aging time, respectively ($W^* = -Ni^* ta^*$, $Conc^* = -Ni^* Ta^*$).

Final properties regarded as relevant to describe the catalyst performance were final nickel content (%Ni), specific surface area (BET), reducibility (%R), metallic surface per gram of nickel ($S_{Ni/gNi}$) and metallic area per gram of reduced nickel (S_{Ni/gNi^0}). Models with the general form of Eq. (1a) are then sought to correlate these variables (hereafter called responses) with the preparation variables.

2.3. Characterization

The nickel content (%) of the catalytic precursors (NiO/SiO₂) was determined by atomic absorption (Perkin Elmer 1100B) after dissolution in a HNO₃/HF solution. Specific surface areas were measured by nitrogen adsorption at liquid nitrogen temperature (77 K) in an ASAP-2000 Micrometrics equipment

after sample outgassing for 2 h, in vacuum. The reducibility was estimated through temperature programmed reduction (TPR). The reduction was carried out in an argon–hydrogen mixture (1.5%) up to 773K, with a heating rate of 10 K/min. The hydrogen consumption during TPR was expressed as a reduction degree (%R), with the assumption that the transition observed is Ni²⁺ to Ni⁰. At the end of a TPR experiment, the metallic dispersion was measured from the adsorption and desorption peaks generated by quickly cooling (823 K down to room temperature) and heating (room temperature up to 773 K) the reduced sample in argon–hydrogen mixture (heating/cooling rates about 100 K/min). Nickel metallic areas were calculated assuming a stoichiometry of 1 H/surface nickel at room temperature. The geometric area of a surface nickel atom was taken as 6.3 Å. The nickel area (S_{Ni/gNi^0}) is referred to the reduced nickel.

3. Results and discussion

Experimental responses are shown in Table 3. Catalysts are labeled in the form wNi_{x-y-z} , where w is the nickel nominal content, x is the precipitation temperature, y is the aging temperature and z is the aging time. A first look on Table 3 shows that the set of preparing conditions gives birth to materials with significantly different properties. The specific surface area of prepared materials ranged from 36 to 327 m²/g and the metallic area per gram of nickel ranged from 10 to 71 m²/gNi.

Estimates for model parameters and parameter variances were obtained with standard linear regression procedures [19]. Standard statistical tests of significance (t -test of student) were used to allow the evaluation of parameter significance. Whenever parameter significance was smaller than 5%, the parameter and respective effect would be removed from Eqs. (1a) and (1b).

The first response analyzed was the final nickel content. Regression results obtained are shown in Table 4.

The model relating the final nickel content and the statically significant preparation variables is:

$$\%Ni_f = (27.4 \pm 0.4) + (11.2 \pm 0.5)Ni^* + (1.7 \pm 0.5)Tp^* + (1.1 \pm 0.5)Conc^*, \quad (2)$$

Table 3
Experiment results^a

No.	Catalysts	Response			
		% Ni	%R	BET (m ² /g)	S _{Ni} (m ² /g Ni)
1	20Ni ₂₉₈₋₂₉₈₋₀	11.4	81	38	60
2	20Ni ₂₉₈₋₂₉₈₋₂₀	17.8	71	45	54
3	20Ni ₂₉₈₋₃₆₃₋₀	9.9	82	36	54
4	20Ni ₂₉₈₋₃₆₃₋₂₀	17.3	23	195	18
5	20Ni ₃₆₃₋₂₉₈₋₀	16.7	90	54	71
6	20Ni ₃₆₃₋₂₉₈₋₂₀	17.8	72	72	40
7	20Ni ₃₆₃₋₃₆₃₋₀	16.9	85	54	52
8	20Ni ₃₆₃₋₃₆₃₋₂₀	19.0	17	229	10
9	40Ni ₂₉₈₋₂₉₈₋₀	36.8	97	54	25
10	40Ni ₂₉₈₋₂₉₈₋₂₀	39.6	98	54	47
11	40Ni ₂₉₈₋₃₆₃₋₀	35.2	97	47	29
12	40Ni ₂₉₈₋₃₆₃₋₂₀	34.4	49	327	25
13	40Ni ₃₆₃₋₂₉₈₋₀	40.4	95	70	29
14	40Ni ₃₆₃₋₂₉₈₋₂₀	41.5	100	81	28
15	40Ni ₃₆₃₋₃₆₃₋₀	40.7	100	57	29
16	40Ni ₃₆₃₋₃₆₃₋₂₀	36.9	50	325	42
17	30Ni ₃₃₀₋₃₃₀₋₁₀	27.3	91	100	44
18	30Ni ₃₃₀₋₃₃₀₋₁₀	30.9	91	134	37
19	30Ni ₃₃₀₋₃₃₀₋₁₀	28.8	85	98	50
20	30Ni ₃₃₀₋₃₃₀₋₁₀	29.4	76	109	38
Maximum		42	100	327	71
Mean		27	81	109	39
Minimum		10	17	36	10

^awNi_{x-y-z}: w is the nominal nickel content, x is the precipitation temperature, y is aging temperature and z is the aging time.

Table 4
Linear regression analysis: results for final nickel content (Ni_f)

	Coefficient (a _i)	Standard error (s)	Level of significance
Independent term	27.4	0.4	>95%
Ni*	11.2	0.5	>95%
Tp*	1.7	0.5	>95%
Ta*	-0.7	0.5	<95%
ta*	1.0	0.5	<95%
W*	0.7	0.5	<95%
Conc.*	1.1	0.5	>95%

so that non-linear effects are not necessary to describe this response. The excellent agreement between the model and the experimental results can be seen in Fig. 2. The error bars were calculated based on the results obtained with the central experiments. Errors were assumed to be constant throughout the experimental region.

From Eq. (2) it may be concluded that the final nickel loading depends mainly on precipitation con-

ditions. The total amount of nickel present in the slurry (nominal nickel content) is, obviously, the more important variable and shows a direct relation with the final nickel content. The remaining precipitation variables, temperature and nickel nitrate concentration also exert a direct influence upon the final nickel content. The influence of the former is related to the increase of the nuclei formation. The influence of the latter is related to the increase of the effective-

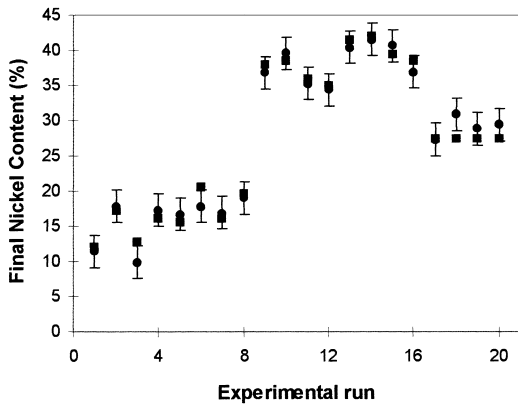


Fig. 2. Comparison between (●) Observed and (■) predicted final nickel contents.

ness of the precipitation due to faster reaching of the conditions of super saturation at higher concentrations. As aging variables are not important to describe the final nickel content, there is no reason to believe that the interaction between nominal nickel content and aging temperature (Ni^*Ta^*) is important in this case.

Similar regression analysis was applied to the other responses. In these cases, however, the interaction between aging time and aging temperature (the most significant variables for specific surface area and reducibility) could not be dropped from Eqs. (1a) and (1b). Estimates for model parameters and parameter standard errors are shown in Table 5.

The final regression equations relating the preparation variables and the responses are:

Table 5
Linear regression analysis. Results for remaining responses.

	BET		%R		$S_{Ni/gNi}$	
	a_i	s	a_i	s	a_i	s
b_i	108.9 ^a	4.3	77.5 ^a	1.5	39.0	1.8
Ni^*	18.3 ^a	4.9	10.3 ^a	1.7	-6.5 ^a	2.0
Tp^*	9.1	4.9	0.7	1.7	-0.7	2.0
Ta^*	50.1	4.9 ^a	-12.6 ^a	1.7	-6.1 ^a	2.0
ta^*	57.4 ^a	4.9	-15.4 ^a	1.7	-5.3 ^a	2.0
W^*	-12.0 ^a	4.9	-0.8	1.7	-5.5 ^a	2.0
$Conc^*$	-12.5 ^a	4.9	-3.9 ^a	1.7	-9.0 ^a	2.0
Ta^*ta^*	52.9 ^a	4.9	-12.7 ^a	1.7	-3.4	2.0

^aStatistically significant effects (level of confidence 95%).

$$\begin{aligned}
 BET = & (108.9 \pm 4.3) + (18.3 \pm 4.9)Ni^* \\
 & + (50.1 \pm 4.9)Ta^* + (57.4 \pm 4.9)ta^* \\
 & + (12.5 \pm 4.9)Conc^* - (12.0 \pm 4.9)W^* \\
 & + (52.9 \pm 4.9)Ta^*ta^*, \quad (3)
 \end{aligned}$$

$$\begin{aligned}
 \%R = & (77.5 \pm 1.6) + (10.3 \pm 1.7)Ni^* \\
 & - (12.6 \pm 1.7)Ta^* - (15.4 \pm 1.7)ta^* \\
 & + (4.0 \pm 1.7)Conc^* - (12.8 \pm 1.7)Ta^*ta^*, \quad (4)
 \end{aligned}$$

$$\begin{aligned}
 S_{Ni} = & (39.0 \pm 1.8) - (6.5 \pm 2.0)Ni^* \\
 & - (6.1 \pm 2.0)Ta^* - (5.3 \pm 2.0)ta^* \\
 & + (5.5 \pm 2.0)W^* - (9.0 \pm 2.0)Conc^*. \quad (5)
 \end{aligned}$$

For these responses, the effect of nominal nickel content, aging time and aging temperature are important so that the effect of their interactions may also be important. This means that if $Conc^*$ is replaced by Ni^*ta^* , and W^* is replaced by Ni^*Ta^* in Eqs. (3)–(5), the same results are obtained. So, calculated effects for nominal nickel concentration ($Conc^*$) and agitation (W^*) cannot be discriminated from interactions between nominal nickel content and aging time (Ni^*ta^*) and between nickel content and aging temperature (Ni^*Ta^*) with this experimental set.

The equations containing both interactions are:

$$\begin{aligned}
 BET = & (108.9 \pm 4.3) + (18.3 \pm 4.9)Ni^* \\
 & - (50.1 \pm 4.9)Ta^* - (57.4 \pm 4.9)ta^* \\
 & + (12.5 \pm 4.9)Ni^*ta^* + (12.0 \pm 4.9)Ni^*Ta^* \\
 & + (52.9 \pm 4.9)Ta^*ta^*, \quad (6)
 \end{aligned}$$

$$\begin{aligned}
 \%R = & (77.5 \pm 1.6) + (10.3 \pm 1.7)Ni^* \\
 & - (12.6 \pm 1.7)Ta^* - (15.4 \pm 1.7)ta^* \\
 & + (3.9 \pm 1.7)Ni^*ta^* - (12.7 \pm 1.7)Ta^*ta^*, \quad (7)
 \end{aligned}$$

$$\begin{aligned}
 S_{Ni} = & (39.0 \pm 1.8) - (6.5 \pm 2.0)Ni^* \\
 & - (6.1 \pm 2.0)Ta^* - (5.3 \pm 2.0)ta^* \\
 & + (5.5 \pm 2.0)Ni^*Ta^* + (9.0 \pm 2.0)Ni^*ta^*. \quad (8)
 \end{aligned}$$

The usual procedure used to discriminate confounded variables is enlarging the original design matrix or running an entirely new experimental design containing only the confounded variables, which means at least eight new experiments in our problem. However, an alternative approach is used here, based on a very simple model discrimination strategy. Mod-

Table 6
Response values obtained with Eqs. (3)–(5) and Eqs. (6)–(8) used for model discrimination

Experiment	Variables						Difference between models		
	Ni*	Tp^*	Ta^*	ta^*	W^*	Conc*	(2)–(5)	(3)–(6)	(4)–(7)
21	–1	–1	–1	–1	–1	–1	0	0	0
22	–1	–1	–1	1	1	1	12	0	11
23	–1	1	1	–1	1	1	13	8	18
24	–1	1	1	1	–1	–1	37	8	29
25	1	–1	1	–1	–1	1	12	0	0
26	1	–1	1	1	1	–1	12	0	11
27	1	1	–1	–1	1	–1	37	8	18
28	1	1	–1	1	–1	1	13	8	7

els constituted by Eqs. (3)–(5) and Eqs. (6)–(8) can be used to predict the output values of the response variables for the eight experimental conditions of the new design matrix built for the confounded variables. Experimental conditions where differences between the two rival models are maximized are then carried out, as shown in Table 6.

As maximum differences between the rival models were found in experiments 23, 24 and 27, these experiments were selected and performed. As shown in Table 7, the model containing the interactions led to much better predictions for all responses, in a very large range of specific surface area, degree of reduction and metallic area, indicating that this is the best model. The agreement between calculated and experimental specific surface area, degree of reduction and metallic area can be seen in Figs. 3–5 for the whole experimental grid. It is important to note that all the calculated values are in very close agreement with the experimental values and within the experimental error.

The final model constituted by Eqs. (6)–(8) seems to indicate that the variables nickel loading, aging time and aging temperature (and their interactions) are the most important ones and determine the main final

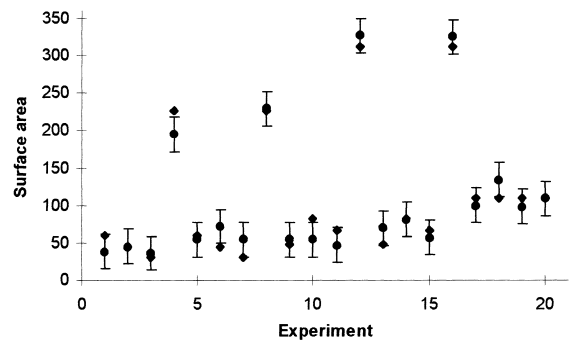


Fig. 3. Comparison between (●) observed and (■) predicted specific surface areas.

catalyst properties, namely specific surface area, reducibility and metallic area. The variables metal loading (concentration of a reactive species), temperature and time are natural variables used to describe the evolution of chemical reactions, suggesting that a chemical reaction may be occurring during the aging step. The formation of nickel silicate during the aging step has already been pointed out by other researchers [20,21]. Formation of nickel silicates [10,11,13] would be responsible for the formation of a new phase on the

Table 7
Experimental and predicted values for response values used for model discrimination

Experiment	BET			%R			S_{Ni}		
	Eq. (3)	Eq. (6)	Experimental	Eq. (4)	Eq. (7)	Experimental	Eq. (5)	Eq. (8)	Experimental
23	264	227	189	79	87	93	30	48	43
24	18	31	54	30	23	16	49	20	14
27	85	48	47	107	99	100	47	29	26

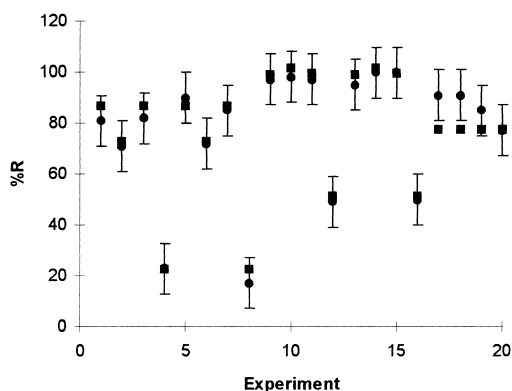


Fig. 4. Comparison between (●) observed and (■) predicted degrees of reduction.

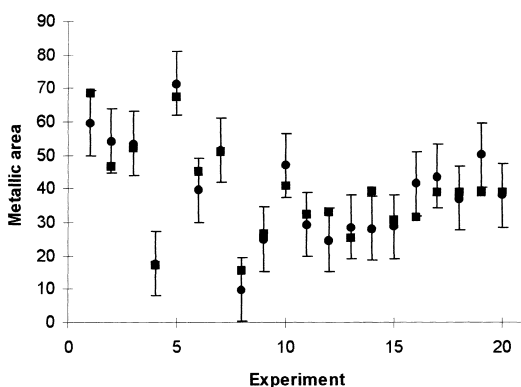


Fig. 5. Comparison between (●) observed and (■) predicted metallic areas.

catalyst, modifying the catalyst texture and increasing the surface area of material considerably. So, the rising of the specific surface area can be related to the nickel antigorita formation, which is favored by higher nickel content, aging temperature and time (which explains the direct relation between nickel loading, aging temperature and time with the specific surface area (BET)).

The decreasing of the reducibility of the catalyst containing silicate supports the assumption of nickel silicate formation, as bulk nickel oxide and nickel with a low metal support interaction are easier to reduce than nickel silicate. Therefore, changes of surface area and reducibility would follow opposite trends. This behavior is described by Eq. (7), which shows an inverse relation between aging time, aging tempera-

ture and reducibility, suggesting that high temperatures and aging time may increase the rate of silicate formation and cause a decrease of the catalyst reducibility (%R). The role of the nickel content is more complex, as nickel may be present as nickel silicate and nickel oxide. At low nickel contents Eq. (7) indicates that the nickel content has a negative effect on catalyst reducibility, which may indicate that most of the nickel present leads to the formation of nickel silicate. However, at high nickel contents, the nickel content has a positive effect on catalyst reducibility, which may indicate that an increasing amount of nickel leads to the formation of nickel oxide, simultaneously increasing the catalyst reducibility.

Eq. (8), which relates metallic nickel surface area and the aging variables, may also be interpreted in terms of a competition between nickel silicate and bulk nickel oxide formation. The metallic area decrease with nickel nominal content would be due to the formation of bulk nickel oxide, which is easily reduced, but produces poorly dispersed metallic nickel. On the other hand, the inverse relation between metallic area and aging time and temperature may be again interpreted in terms of nickel silicate formation, which is hardly reducible. The interactions between nickel loading and aging time and temperature, however, indicate that these variables may be fine tuned in order to allow the production of larger metallic areas, improving the metallic nickel dispersion caused by the nickel silicate formation.

In order to eliminate the effects related to the reduction step from our analysis – the formation of different nickel species with different reactivities towards hydrogen – the analysis is continued in terms of metallic surface area per gram of metallic nickel (S'_{Ni}).

The metallic surface area per gram of metallic nickel (S'_{Ni}) can be obtained by dividing the metallic area per gram of nickel by the degree of reduction (Eqs. (7) and (8)):

$$S'_{Ni} = \frac{S_{Ni}}{\%R}. \quad (9)$$

The behavior of the metallic area per gram of Ni^0 predicted by Eq. (9) was found to be very interesting. At high nickel concentrations, aging at low temperature does not lead to significant changes of the metallic area because the temperature is too low for reaction to

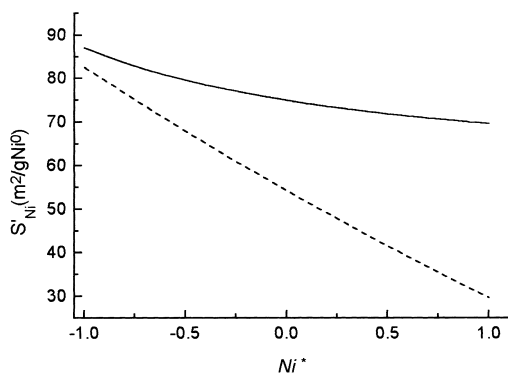


Fig. 6. Effect of aging at high temperature ($Ta^* = 363$ K) and long time ($ta^* = +1$) (—) and no aging (----) on the metallic surface area per gram of $Ni^{(0)}$ at different nominal nickel concentrations.

take place at any significant extent. However, at high temperatures the aging step causes an exponential increase of the metallic area as the aging time increases, demonstrating the positive effect of the nickel silicate formation on the metallic nickel dispersion.

The metallic area of the catalyst can be controlled solely by the precipitation step, if no aging step is carried out (Fig. 6). At no aging ($ta^* = -1$, $Ta^* = +1$) the metallic area is high at low nickel concentration and decreases fast as the nickel loading increases. In this situation, the metallic area is strongly controlled by the nickel content (which can be tuned by the precipitation conditions). If the catalyst is aged, e.g. at 363 K ($Ta^* = +1$) and during 20 h ($ta^* = +1$), the effect of nickel is not only associated with the precipitation step but also with the nickel silicate formation. This way, the deleterious effect of increasing nickel loading during the precipitation step on the metallic area is compensated by the silicate formation, also dispersing the more reducible nickel species. It is interesting to observe the effect of aging time on the metallic area (S'_{Ni}) (Fig. 7). At low temperatures, aging time does not produce appreciable changes on the catalyst metallic area, while at high temperatures the change on the catalyst surface area is dramatic. This effect is due to the slow reaction rates of silicate formation at low temperatures.

In order to find the maximum metallic area per gram of reduced nickel (S'_{Ni} (m^2/gNi^0)), Eq. (9) was maximized in the experimental region of interest. Two

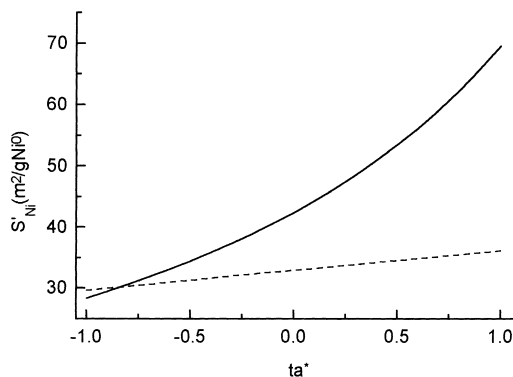


Fig. 7. Effect of aging time (ta^*) at high (—, $Ta^* = 363$ K) and low (----, $Ta = 298$ K) aging temperatures on the metallic surface area per gram of $Ni^{(0)}$ of a high nominal nickel concentration catalyst ($Ni^* = +1$).

close maximum values (with and without aging, as shown in Table 8) may be found at low nickel concentrations. This means that at low nickel concentrations high metallic area can be achieved during the precipitation step; otherwise, similar results can be achieved by tuning the aging conditions. As it can be seen, model predictions are confirmed experimentally. It is worth mentioning that the common feature for both samples is the absence of microporosity and good accessibility to the metallic sites (average diameter pore, dp , above 50 \AA as shown in Table 8).

If similar metallic areas (within experimental error) may be obtained with and without the aging step, from the industrial catalysis point of view it seems that the aging of the precursor may be a waste of time and that the precipitation conditions must be carefully controlled. Besides, the catalyst prepared without aging can be reduced more easily, leading to economy of energy in the process. On the other hand, if the catalyst is prepared to be used in demanding environments (which favors metallic sinterization), aging may be very helpful because it produces nickel species that are more stable to sintering. This is not the case of edible oil hydrogenation. Another point that should be mentioned is that the metallic area increases sharply as the nickel content decreases; therefore, substantially higher metallic area are expected at lower nickel contents.

In order to obtain more insights on the silicate formation, a simple model was developed based on more than statistical foundations. Let us represent the

Table 8
Optimized catalysts^a

Variables			Predicted			Experimental			
Ni*	Ta*	ta*	%R	S'Ni (m ² /gNi)	S'Ni (m ² /gNi ⁰)	%R	SNi (m ² /gNi)	S'Ni (m ² /gNi ⁰)	d _P (Å)
-1	+1	+1	23	20	87	24	18	73	61
-1	-1	-1	86	71	83	81	60	73	99

^aThe remaining variables (Conc*, T_p* and W*) were kept at their -1 level.

reaction of silicate formation by



where Ni represents the nickel species, Sup is the support and P is the reaction product, the silicate. Assuming that this reaction follows a first-order kinetics regarding the nickel concentration and unknown order (*n*) regarding the silica concentration, the rate of silicate formation may be described as

$$\frac{dP}{dt} = k'[\text{Ni}'][\text{Sup}]^n. \quad (11)$$

The support concentration was constant in all preparations, so that it can be grouped with the original kinetic constant. As the real nickel concentration (Ni') in the solution is not known, it is assumed that the nickel concentration is proportional to the catalyst nickel loading. This additional unknown proportionality constant may also be grouped with the original constant *k'*. So, Eq. (11) becomes

$$\frac{dP}{dt} = k[\text{Ni}]. \quad (12)$$

The nickel is consumed during the nickel silicate formation, so that its concentration should not be regarded as constant.

The nickel consumption may be written as

$$\frac{d\text{Ni}}{dt} = -k[\text{Ni}]. \quad (13)$$

The integration of this equation gives us the nickel concentration during the reaction

$$\text{Ni} = \text{Ni}_0 \exp(-kt), \quad (14)$$

where Ni₀ is the total initial nickel loading in the catalyst and *t* is the reaction time. If Eq. (14) is inserted into (Eq. (12)), after integration the resulting

equation is

$$P = \text{Ni}_0 \left[1 - \exp\left(-A \exp\left(\frac{\Delta E}{RT}\right)t\right) \right], \quad (15)$$

where *A* is the pre-exponential factor; Δ*E* is the activation energy; *R* is the universal gas constant, and *T* is the reaction temperature.

It is difficult to measure the amount of silicate produced, so that the catalyst surface area will be used to infer the amount of silicate formed. Let us assume that the final surface area may be described as a sum of two terms: the initial surface area of the catalyst and a contribution that depends on the amount of silicate formed. Then assuming that a linear relationship is valid

$$\text{BET} = S_0 + \alpha P, \quad (16)$$

where *S*₀ is the catalyst initial specific surface area, and α is a proportionality constant. Substituting Eq. (15) into Eq. (16)

$$\text{BET} = S_0 + \alpha \text{Ni}_0 \left[1 - \exp\left(-A \exp\left(\frac{\Delta E}{RT}\right)t\right) \right]. \quad (17)$$

The initial catalyst area may be approximated by the carrier surface area or estimated as an additional parameter of Eq. (17). Both procedures lead to very similar results; therefore, it is preferred here to use the surface area of the carrier as the catalyst initial surface area (*S*₀=42 m²/g).

The activation energy obtained by non-linear regression was equal to 12.2 kcal/mol, a value that lies within the range of expected values for chemical reactions. The parameter α was found to be 9, which explains the sharp increase in the surface area of the catalyst. At high temperatures, as time increases Eq. (17) approaches an asymptote (Figs. 8 and 9),

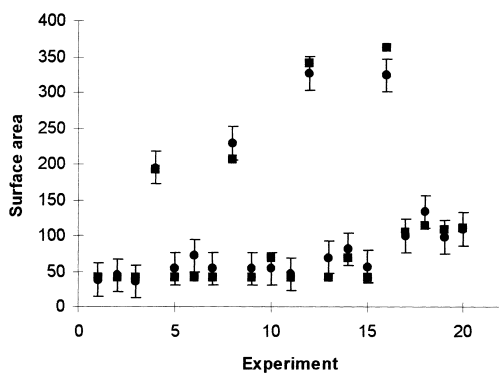


Fig. 8. Comparison between the values (●) observed and (■) predicted by the phenomenological model.

indicating that large specific surface areas may be obtained at aging times smaller than 15 h and that aging times larger than 15 h do not produce appreciable changes on the surface area. At low temperatures, the surface area increases linearly and slowly with time (Fig. 10). The assumption of constant nickel concentration during the reaction was checked; however, it led to significantly poorer results, indicating that the amount of nickel consumed during the reaction is significant and must be taken into account. The agreement between the surface area calculated by the Eq. (17) and the experimental results is very good and can be checked in Fig. 8.

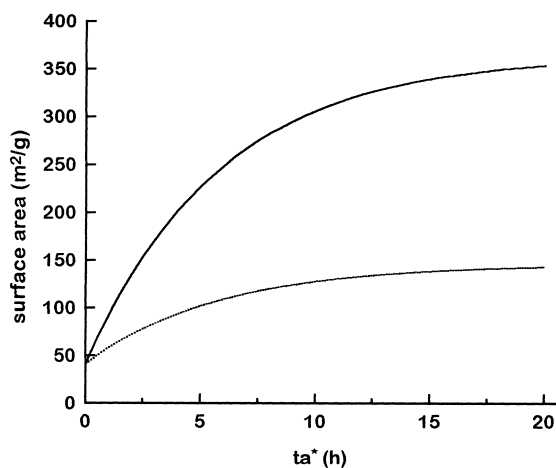


Fig. 9. Surface area evolution at high temperatures: (—) high nickel content $Ni^* = +1$; low nickel content (\cdots) $Ni^* = +1$.

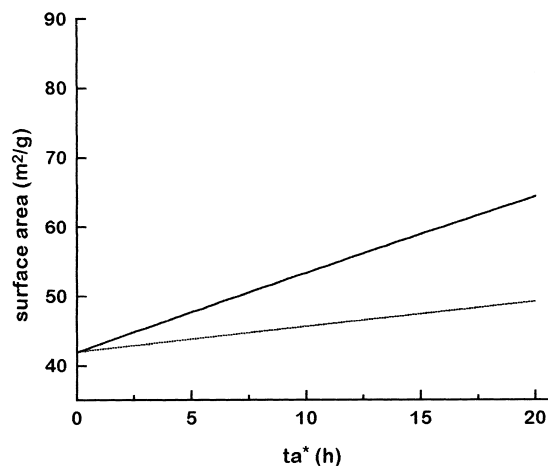


Fig. 10. Surface area evolution at low temperatures: (—) high nickel content $Ni^* = +1$; (\cdots) low nickel content $Ni^* = +1$.

Although this is a very simple model (17), based on some strong hypothesis, it gives some interesting clues on the phenomena that take place during the aging step. However, more fundamental experimental results are needed to validate the model proposed here.

4. Conclusions

Statistical experimental design was used to study the preparation variables related to the precipitation and aging step simultaneously. It was found that the aging step is of fundamental importance for the final catalyst properties, if silicate formation takes place at significant extents. This reaction is favored by high aging temperatures, aging times and nickel loadings. At low temperatures, silicate formation does not take place at significant rates and does not change significantly the catalyst properties.

The behavior of the metallic area per gram of nickel was found to be very interesting. Two different maximum metallic areas can be attained: at strong aging conditions ($ta = +1$, $Ta = +1$) and at no aging. The results were confirmed experimentally, demonstrating that high metallic areas may be obtained during the precipitation step, so that the aging step can be avoided if the precipitation step is carried out carefully and the catalyst is to be used in warm reaction conditions (e.g. edible oil hydrogenation). Otherwise aging may be very helpful to produce more stable

nickel species and adjusting the final catalyst properties.

A very simple phenomenological model was successfully developed to describe some important features of the reaction phenomena, indicating that the surface area approaches an asymptote as aging temperature and aging time increase. Slow changes of the surface area may be expected at low temperatures.

Acknowledgements

The authors thank CNPq – Conselho Nacional de Pesquisa e Desenvolvimento Tecnológico – and CAPES – Conselho de Aperfeiçoamento de Pessoal de Ensino Superior – for providing scholarships and supporting our work.

References

- [1] M. González, O. Gutiérrez, O.E. González, J.A. Delgado, J.R.G. Velasco, *Appl. Catal. A* 162 (1997) 269.
- [2] M. González, O. Gutiérrez, O.E. González, J.R.G. Velasco, *J. Molec. Catal. A* 120 (1997) 185.
- [3] A. Gil, A. Díaz, L.M. Gandía, M. Montes, *Appl. Catal. A* 109 (1997) 167.
- [4] M. Che, Z.X. Cheng, C. Louis, *J. Am. Chem. Soc.* 117 (1995) 2008.
- [5] G.C.A. Schuit, L.L. van Reijen, *Advances in Catalysis*, Academic Press, New York, 1958.
- [6] J.W.E. Coenen, B.G. Linsen, in: B.G. Linsen (Ed.), *Physical and Chemical Aspects of Adsorbents and Catalysts*, Academic Press, New York, 1970.
- [7] J.W. Coenen, in: B. Delmon, P. Grange, P.A. Jacobs, G. Poncelet (Eds.), *Preparation of Catalysts II*, Elsevier, Amsterdam, 1979.
- [8] A.M. Hermans, J.W. Geus, in: B. Delmon, P. Grange, P.A. Jacobs, G. Poncelet (Eds.), *Preparation of Catalysts II*, Elsevier, Amsterdam, 1979, p. 113.
- [9] J.W. Geus, in: B. Delmon, P. Grange, P.A. Jacobs, G. Poncelet (Eds.), *Preparation of Catalysts III*, Elsevier, Amsterdam, 1983, p. 1.
- [10] V.M.M. Salim, M. Schmall, R. Frety, M.M. Rodrigues, M.S. Silveira, in: *Reprints of the Fifth Brazilian Seminar on Catalysis*, IBP (Ed.), Guarujá, 1989.
- [11] A.F. da Silva Jr., V.M.M. Salim, M. Schmall, R. Frety, in: B. Delmon, P. Grange, P.A. Jacobs, G. Poncelet (Eds.), *Preparation of Catalysts V*, Elsevier, Amsterdam, 1991.
- [12] V.M.M. Salim, D.V. Cesar, M. Schmall, M.A.I. Duarte, R. Frety, in: B. Delmon, P. Grange, P.A. Jacobs, G. Poncelet (Eds.), *Preparation of Catalysts VI*, Elsevier, Amsterdam, 1995.
- [13] C.C. Augusto, C.A. Perez, H.S. Amorim, L.C. Dieguez, V.M.M. Salim, in: *Reprints of the Eighth Brazilian Seminar on Catalysis*, IBP (Ed.), Nova Friburgo, 1995.
- [14] C.O. Rouiller, J.M. Assaf, *Chem. Eng. Sci.* 51 (1996) 2921.
- [15] E. Baker, R. Burch, S.E. Golunski, *Appl. Catal.* 53 (1989) 279.
- [16] A.G. de Lima, M. Nele, E.L. Moreno, H.M.C. de Andrade, in: *Reprints of the Eighth Brazilian Seminar on Catalysis*, IBP (Ed.), Nova Friburgo, 1995.
- [17] E.A. Dawson, P.A. Barnes, *Appl. Catal. A* 90 (1992) 217.
- [18] P.J. Ross, *Taguchi Methods for Quality Engineering*, McGraw-Hill, New York, 1988.
- [19] G.E.P. Box, W.G. Hunter, J.S. Hunter, *Statistics for Experimenters*, Wiley, New York, 1978.
- [20] J.W.E. Coenen, *Appl. Catal.* 75 (1991) 193.
- [21] P. Burattin, M. Che, C. Louis, *J. Phys. Chem. B* 101 (1997) 7060.